

APPLICATION OF REMOTE SENSING DATA FOR ENVIRONMENTAL MONITORING IN SEMIARID MOUNTAIN AREAS: a Case Study in Yemen Mountains

Ayoub Almhab

Department of Remote Sensing, Faculty of Geoinformation Science and Engineering
Universiti Teknologi Malaysia, 81310 Skodai, Johor, Malaysia
e-mail: aalmhap@maktoob.com

ABSTRACT

Remote sensing has been proved to be a very useful technology in the investigation of surface parameters and environment monitoring when large areas is covered. In this paper, the complementarily between two optical remote sensing data Landsat TM and Radar Sat (DEM) were used to estimate and describes the affected surface temperature by elevation, slope and aspect of the land surface, in additional to effect of solar radiation on surface temperature and relation of elevation to wind speed. The two important factors related temperature difference near surface (dT) function is the relationship between wind speed and the surface temperature, and the change of the temperature difference near surface dT function for each image was investigated. The information in this paper provides good background for Remote Sensing applications for monitoring the environment especially in the mountainous areas.

An application for computing temperature map over Sana'a Basin in central mountainous in Yemen is presented.

Keywords: Remote Sensing; Semiarid; LANDSAT TM; Radar Sat; DEM; Yemen.

2. Introduction

The land surface temperature (ST) is an important factor that controls most of the physical, chemical and biological processes in the Earth. Knowledge of the ST is necessary for many environmental studies and management activities of the Earth surface resources (Li & Becker 1993).

It is possible to obtain the radiance data from space-borne devices by recording of the emitted energy directly from the earth surface. In order to obtain this parameter from space radiometry in the thermal infrared part of the eletromagnetic spectrum, it is necessary to take into account emissivity and to correct the recorded signal for the perturbations created by the atmosphere along the path between the Earth's surface and the sensor (Becker & Li, 1990).

This paper describes how surface temperature is affected by elevation, slope and aspect of the land surface. The information in this paper provides good background for correlation of surface parameter, needed for the architectural design, especially in mountain areas.

3. Methodology

3.1. Study area

The Sana'a Basin is located in the western highlands of Yemen. It is opposite the Red Sea and the Gulf of Aden as can be seen in (figure 1A). It is mostly an intermountain plain surrounded by highlands from the west, south and east. On a regional scale, the Basin extends across the central part of the Sana'a (figure 1B) and covers about 24% (3250 km²) of its total area (13,550km²).

There is significant variation in altitude both east-west and north-south extends. The highest point in the Basin is in the southwest end (Jabal An Nabi Shu'ayb) and has an elevation of almost 3700 m above sea level (m.s.l.) The lowest (about 1900 m.s.l.) is in the northern extremity where the Wadi Al Kharid exits the Basin towards the main basin by the same name. The predominant climate is arid although semi-arid conditions prevail in localized areas, particularly along the western highlands, Yemen.

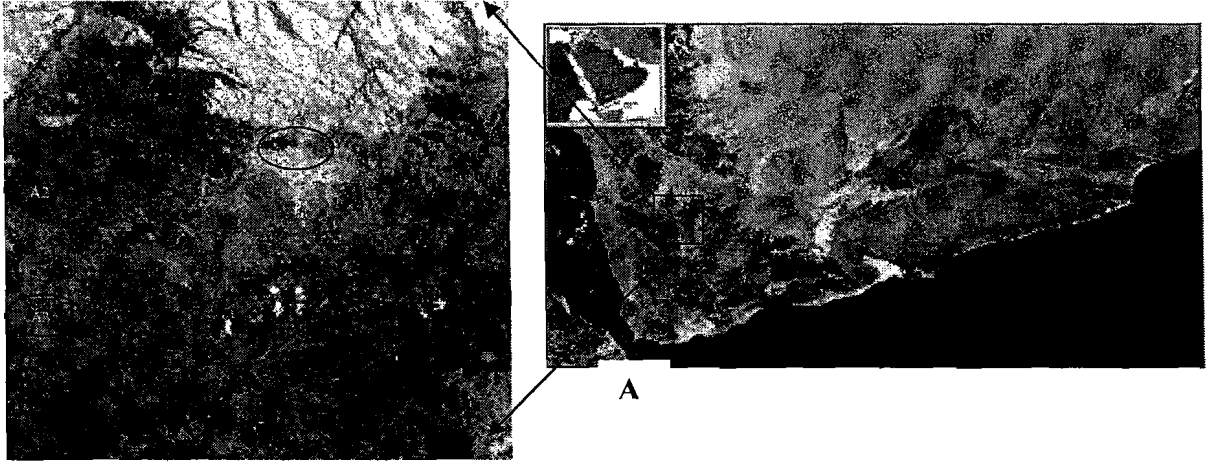


Figure 1A, B: location of Sana'a Basin Yemen Mountains and the three sample areas, (true color image of Landsat 5, image dated 6/01/98.

3.2 Location of the sample areas used for analysis

Three mountainous areas in Landsat Path/Row 40/39 (Figure 1B) were selected for investigating the surface temperature behavior in mountain regions. In figure 1, Area 1, north Sana'a, Sparse vegetation at relatively low elevation. Area 2 has relatively high elevation but not high enough. Area 3, just west of Sana'a, is mainly composed of southeast and northwest facing slopes, with some agriculture vegetation in the northwest side of the mountains. Each of the sample pixels was randomly selected from the three areas. The surface temperature behavior in mountain areas was analyzed using the selected sample pixels.

Each 10-sample~ pixels areas randomly selected from the three areas. The surface temperature behavior in mountain areas was analyzed using the selected 30 sample pixels. Data from the field measurement area were available to assist in calculate of the temperature at locations with in the study area (Lat: 15.3 N, long: 43.15 E). The ERDAS-IMAGINE 8.5 software package was used in this study.

The estimated value of surface temperature, aspect, solar zenith angle and net radiation from remote sensing data LANDSAT TM, were used after (Almhab et al, 2007a,b,c).

4. Results and discussion

4.1 Effect of solar radiation on surface temperature

Surface temperature (ST) in a mountain area is definitely affected by the intensity of the incoming solar radiation. If ST is plotted vs land surface aspect angle, a clear sine curve, with the top of the curve at around the instantaneous sun azimuth angle, is obtained (Figure 2). This is primarily because the average instantaneous incoming solar radiation is the strongest at the instantaneous sun azimuth angle.

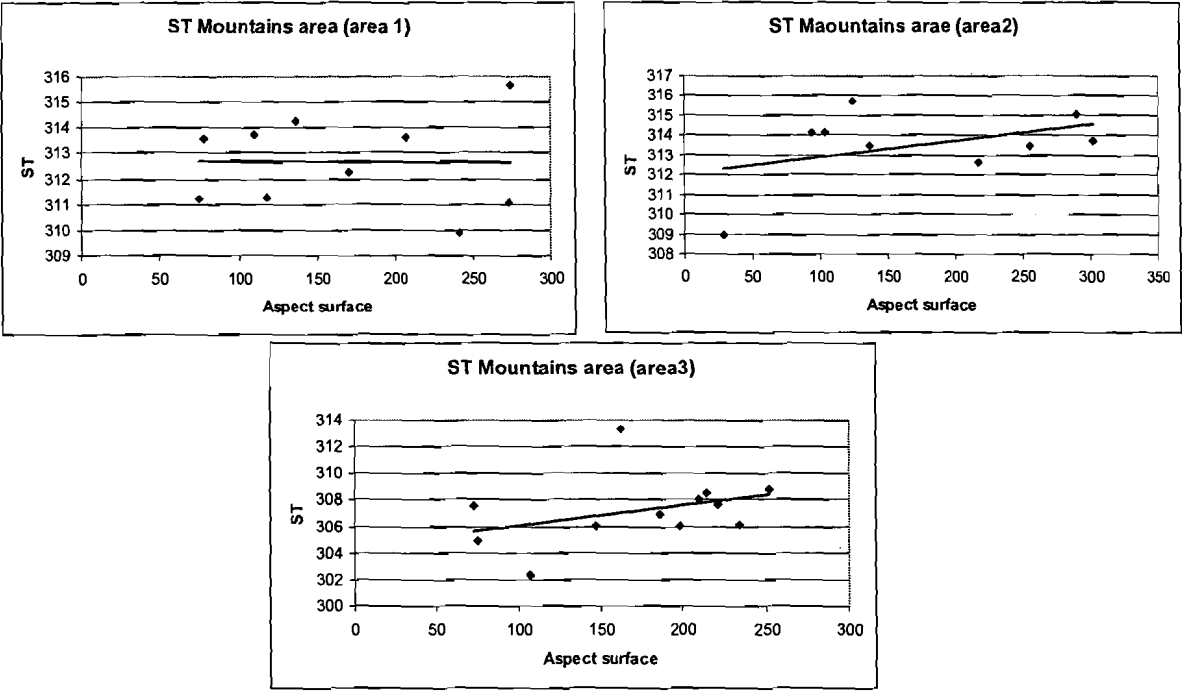


Figure2. ST versus surface aspect angle for the three sample areas, 6/012/98. Sun azimuth angle for the satellite time (10:21am, in solar time) was 51°.

There is about a 10 °C "width" in each sine curve. This variation of 10 ° thy are within a specific surface aspect angle would be from a combination of many factors - difference of surface slope intensity, windspeed difference, different landuse and soil structure/texture condition, topographical difference, elevation difference, and so on. The mean amplitude change in the sine curve was about 15 °C between 135° and 315° aspect for image data dated 6/01/98. This type of sine curve was observed not only for 6/01/98 but also for all other images from June to September (see, Figure.3). Unfortunately, the periods from January to May and from October to December could not be analyzed due to hazy nature of the atmosphere around the mountains.

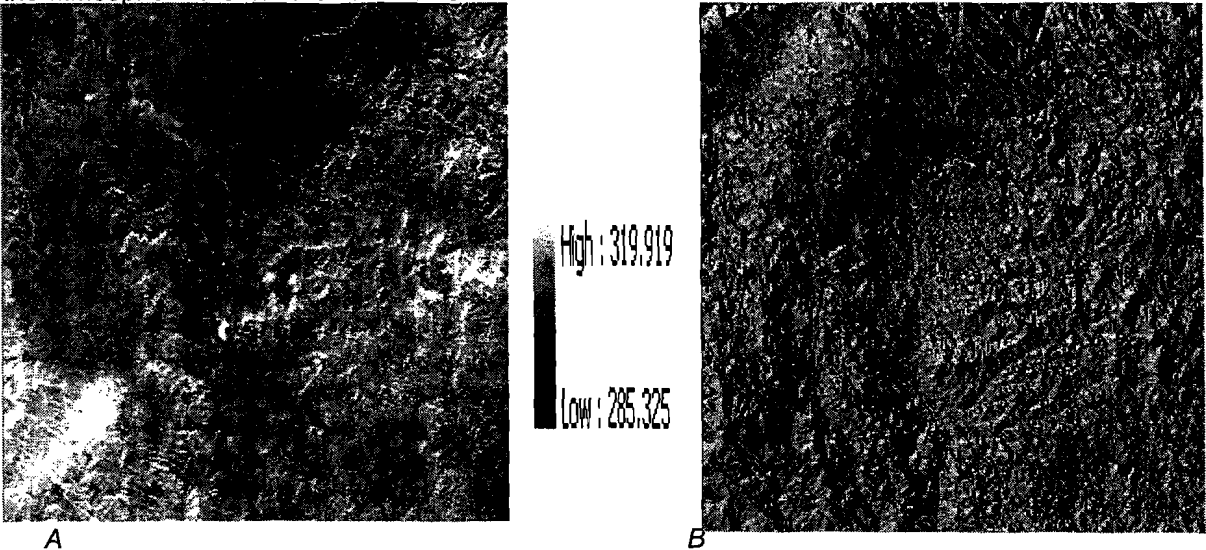


Figure.3A,B. surface temperature(A) (left) versus surface aspect angle B(right) for the Area 1 6/01/98

The sine relationship between surface temperature and surface aspect is as shown in figure 3 A,B. Also, the intensity of slope for each surface has not taken in to consideration. Cosine of solar incident angle ($\cos\theta$) is a more appropriate term to explain the effect of instantaneous solar radiation. The following graphs represent the relationship between ST and $\cos\theta$. $\cos\theta$ generally cannot be more than 1. The $\cos\theta$ values in Figure 4 are in a "horizontal equivalent", which is calculated as $\cos\theta/\cos(\text{surface slope})$. Therefore, $\cos\theta$ can take values more than 1.

As it can be seen that $\cos\theta$ has linear relationship with the instantaneous solar radiation (in a clear sky condition). Therefore, the linear relation between surface temperature and $\cos\theta$ in Figure 4 indicates that surface temperature and incoming solar radiation have a linear relationship.

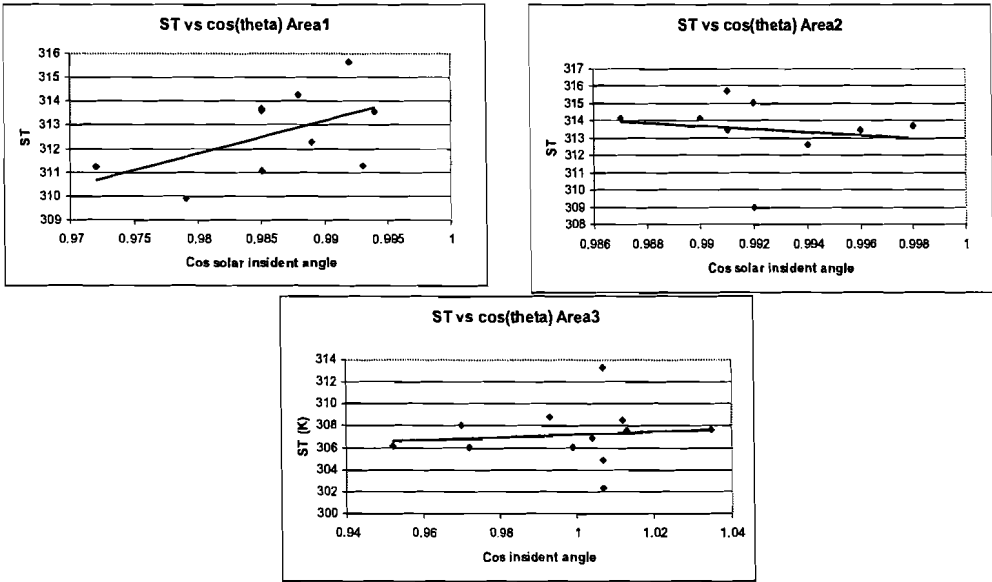


Figure4. ST versus $\cos\theta$ (horizontal equivalent) for the three sample areas.

The intensity of solar radiation strongly affects the net radiation (R_n). Therefore, a similar trend can be observed in ST versus R_n graphs.

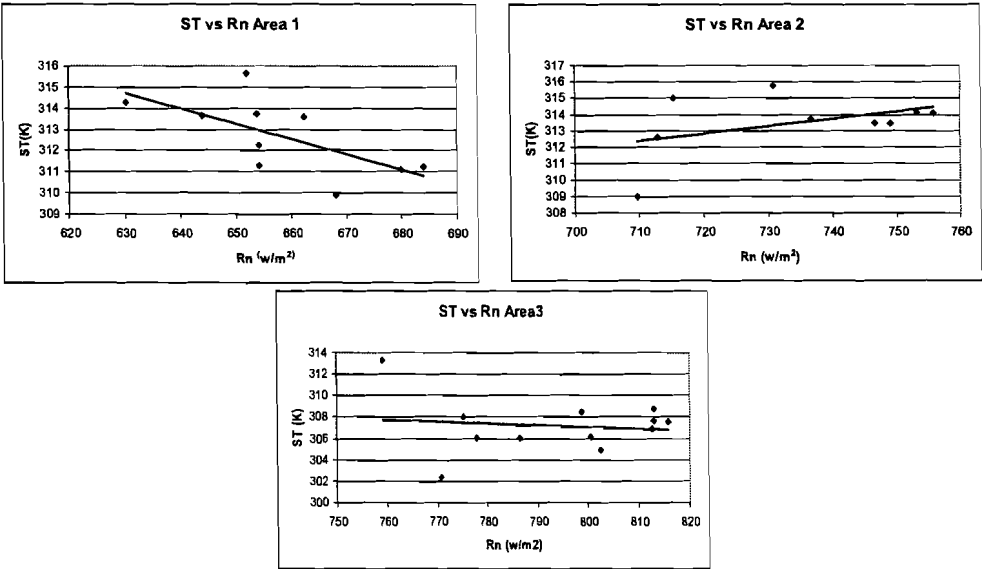


Figure 5. ST vs instantaneous R_n for the three sample areas, image dated 6/01/98

Also, surface temperature at 10:21am shows some trend with 24-hour extraterrestrial solar radiation. This trend would be more clear if the instantaneous T_s was taken at noon, and less clear if the instantaneous T_s was taken at early morning or late evening.

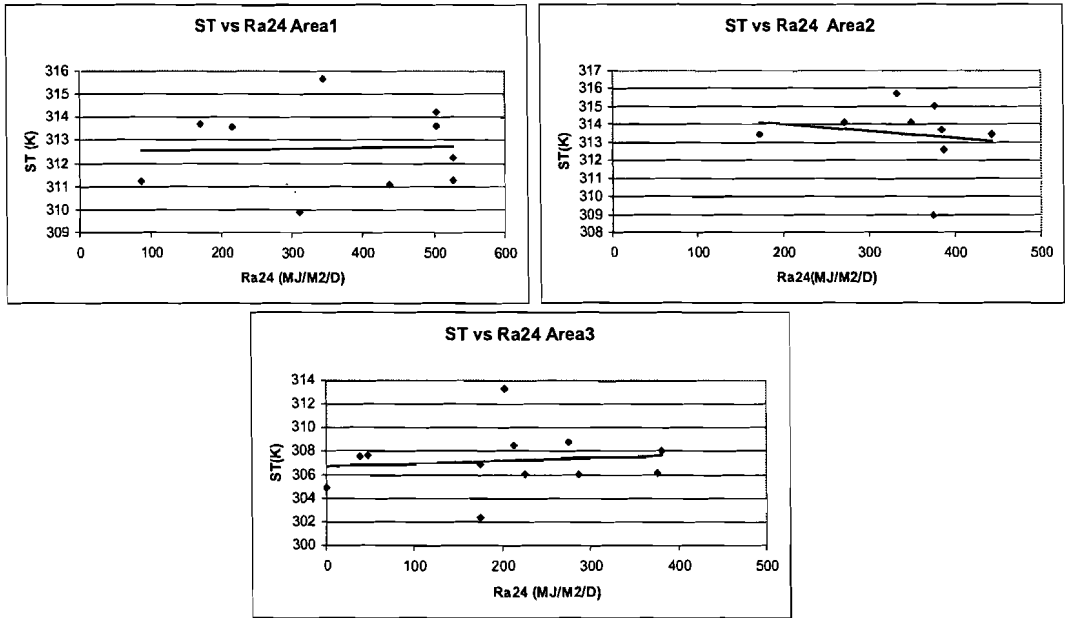


Figure 6. Instantaneous ST versus 24-hour extraterrestrial solar radiation ($R_a(24)$) for the three sample areas, 6/01/98.

4.2 Effect of elevation on surface temperature

Air temperature for standard moist air mass decreases at a lapse rate of $6.5^{\circ}\text{C}/\text{km}$. This lapse effect can be explained by the relation among elevation, air pressure, air temperature and vapor holding capacity of air. Lapse effect of air would have a directly impact on the land surface temperature. Consequently, at higher elevations, colder air temperature due to the lapse effect reduces the surface temperature.

The following graphs show the plots of ST vs Elevation for the three sample areas.

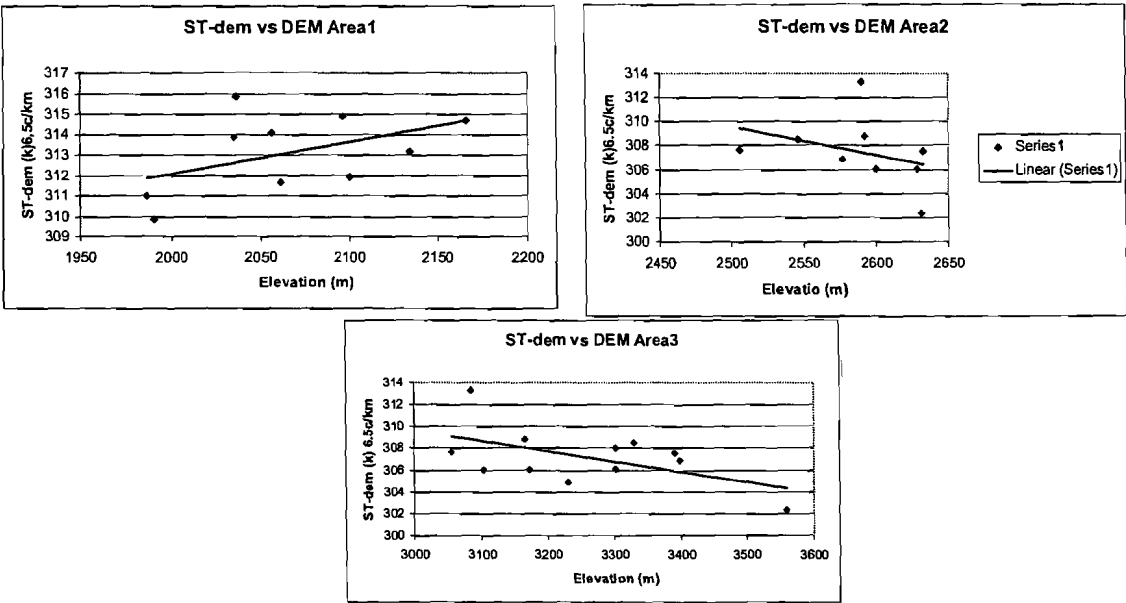


Figure7. Elevation versus Instantaneous ST for the three sample areas, image dated 6/01/98.

All three sample areas show that higher elevation land surfaces will tend to have a lower surface temperature. One reason for this observed trend is the lapse effect of air as described above. The lapse effect is not necessarily the only reason for the decrement of surface temperature, since a similar trend is expected if windspeed, soil moisture and/or landuse are correlated to the elevation. The range in surface temperature for a specific elevation is large, because the incoming solar radiation (described in the previous section) is a stronger factor for ST in mountain areas. Figure 8 shows the DEM adjusted surface temperature ($ST_{(DEM)}$), assuming that the elevation effect is $6.5^{\circ}\text{C}/\text{km}$ (same as the air lapse rate). By this adjustment, the surface temperatures become almost independent of elevation. This may indicate that the lapse rate of surface temperature is similar to the air lapse rate.

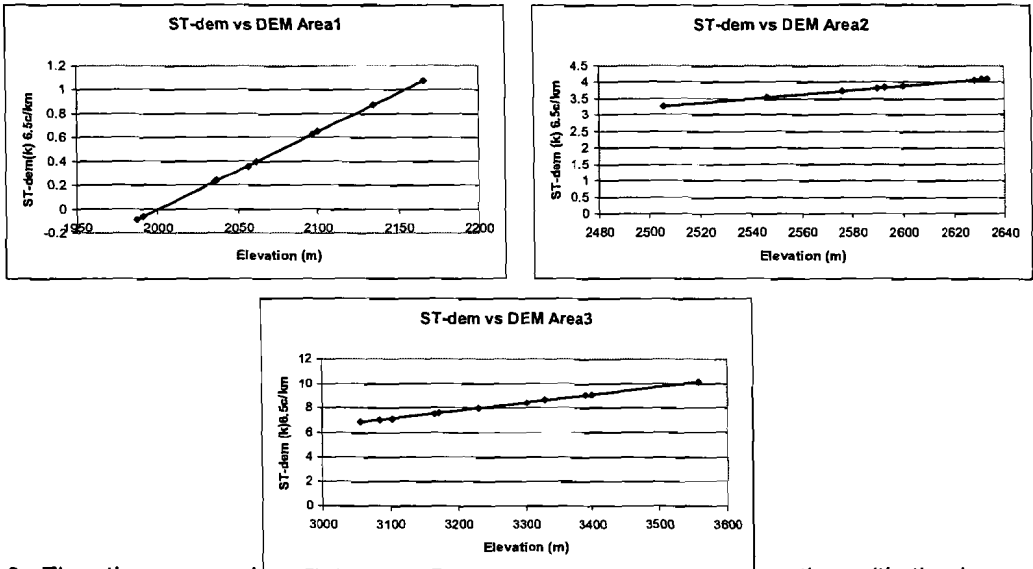


Figure8. Elevation versus instantaneous adjusted ST (adjusted by elevation with the lapse rate) for the three sample areas, image dated 6/01/98.

Figures 9 show the effect of ST adjustment by DEM in June images. Similarly to Figure .8 (June), DEM adjusted surface temperature is almost independent of elevation, both in June and September.

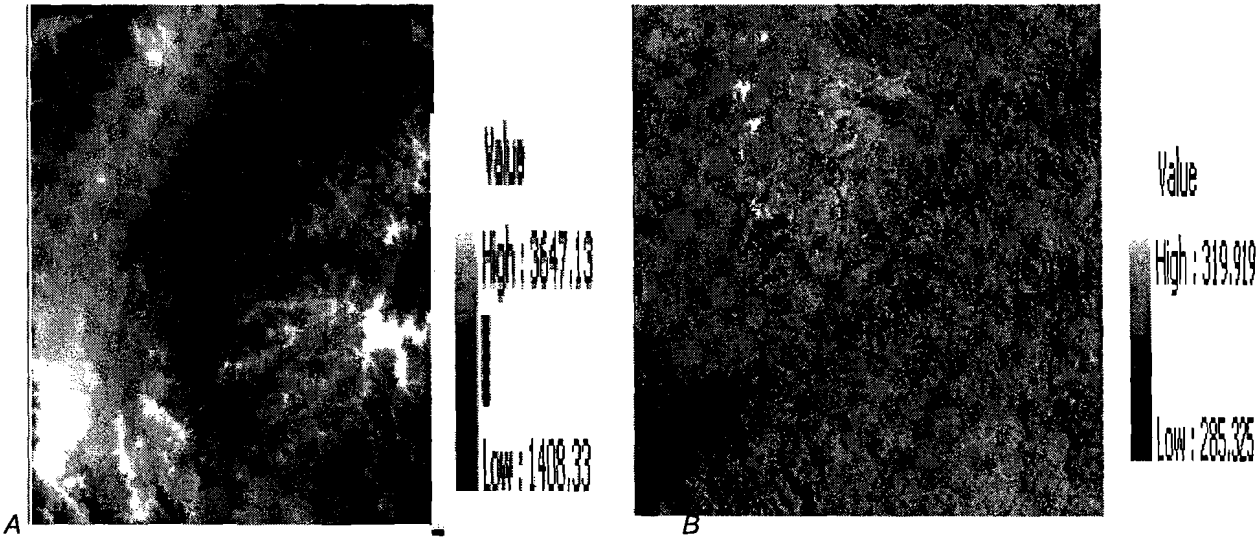


Figure 9A,B. Elevation (A-left) versus instantaneous ST (B-right) for the sample areas image dated 6/01/98.

4.3 Relations of elevation to wind speed

In mountainous areas, lapse corrected surface temperature was almost independent of elevation as shown in figures 7, 8, and 9. If windspeed affects the surface temperature as, the results from Figures 7 to 10 indicate that effects of windspeed on T_s are almost independent of elevation in mountain areas (or error in lapse rate for the surface temperature is affected by the actual trend of windspeed with elevation).

It is likely that windspeed is not a strong function of elevation in mountainous regions. Essentially, windspeed increases when elevation increases from the base (Oke, 1987). However, windspeed is a strong function of the shape of terrain and the direction of windspeed, for a specific land surface (Oke, 1987, and Kaimal and Finnigan, 1994). Therefore, in mountainous areas, windspeed should be a strong function of the wind direction and surface aspect angle rather than elevation itself. Namely, the upwind surface of a mountain has higher wind but the opposite side might be calm. Although one should expect some windspeed increase with elevation in mountains due to the Venturi effect and closer proximally to upper air streams, the general increase appears to be too small to discuss accurately from the surface temperature data.

4.4 Estimation related temperature difference near surface (dT)

The objective of the study is to compute the Temperature maps using only remote sensing data. A problem is then to estimate air temperature without available meteorological stations. To solve this problem, propose to replace the temperature gradient between soil and air by a linear function of ΔT .

$$\Delta T = ST - T_{air} = a \times ST + b \tag{Eq. 1}$$

Where:
 ST is surface temperature, T_{air} is air Temperature, a , b is experimental constants obtain daily maps of ST at the chosen scale.

The computing daily maps of ST and T_{air} by using only satellite data, we have proposed to replace the gradient of temperature by a linear function of $\Delta T = ST - T_{air}$
 $= a ST + b$.
 Simultaneous measurements of T_{air} and ST have been collected during a field-trip and a linear regression has been achieved to obtain the following relation (equation 2 and 3), figure 10A,B :

$$\Delta T = ST - T_{air} = -0.76 \times ST + 28.08 \tag{Eq. 2}$$

and $T_{air} = ST + \Delta T$

$$T_{air} = \Delta T + ST = a \times ST + b = 0.74 \times ST + 8.43 \tag{Eq. 3}$$

with a correlation coefficient of $r^2=0,87.3$.

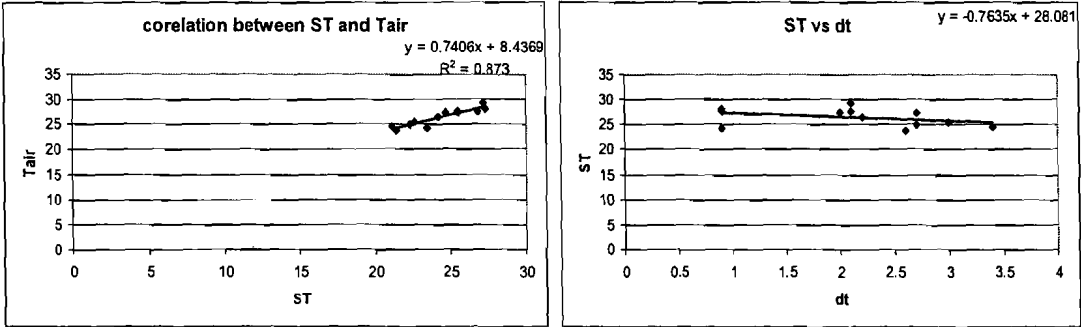


Figure10. Air Temperature (T_{air}) versus ST (A) (left) ST vs temperature difference near surface (dt) B(right) for the sample areas.

5. Conclusion

Computed map of surface temperature ST has been carried from Landsat TM, that a thermal channel with a suitable spatial resolution of $90\text{ m} \times 90\text{ m}$. The simulation result is very much similar to the measurement taken under stressed and no stressed conditions. This study has been able to demonstrate that the surface parameters can be accurately derived from satellite image data. In this case surface parameters that have been derived from LANDSAT 5 TM images data captured surface parameters are validated to gauge the accuracy.

6. References

Almhab et al, 2007a. Estimation of regional scale evapotranspiration for arid area using NOAA-AVHRR application in republic of Yemen, MAPASIA2007, Kula Lumpur , Malaysia.

Almhab et al, 2007b. Estimation of regional evapotranspiration for Arid Areas Using LANDSAT Thematic Mapper Images data: A Case Study for Grape Plantation, ISG & GPS/GNSS 2007, Johor ,Malaysia

Almhab et al, 2007c. Comparison of regional evapotranspiration using NOAA-AVHRR and LANDSAT-TM images: a case study in an arid area in the Sana'a basin, republic of Yemen, Middle East spatial technology 4th conference & exhibition, Al- Bahrain Kingdom.

Kaimal.J.C. and J.J.Finnigan, 1994. Atmospheric Boundary Layer Flows: Their Structure and Measurement. Oxford University Press, NY

Oke,T.R, 1987. Boundary Layer Climates. Routledge, NY

Tasumi, M., Bastiaanssen, W.G.M. and Allen, R.G., 2000, Application of the EBAL methodology for estimating consumptive use of water and stream flow depletion in the Bear River Basin of Idaho through remote sensing. EOSDIS Project Final Report, Appendix C.